Photophysics of Soret-Excited Tetrapyrroles in Solution. I. Metalloporphyrins: MgTPP, ZnTPP, and CdTPP

Umakanta Tripathy, Dorota Kowalska, Xia Liu, Suresh Velate, and Ronald P. Steer*

Department of Chemistry, University of Saskatchewan, 110 Science Place Saskatoon, SK Canada S7N 5C9

Received: February 16, 2008; Revised Manuscript Received: April 2, 2008

The photophysical behavior of three Soret-excited diamagnetic meso-substituted tetraphenylmetalloporphyrins, MgTPP, ZnTPP, and CdTPP, have been examined in a wide variety of solvents using both steady-state and femtosecond fluorescence upconversion methods. The S_2 population of MgTPP decays to S_1 on the time scale of a few picoseconds with unit S_2–S_1 internal conversion efficiency, and the decay rates conform to the weak coupling case of radiationless transition theory. The energy gap law parameters characterizing the coupling of the S_2 and S_1 states of MgTPP have been obtained. The most important accepting vibrational modes in the S_1 state are multiple in-plane C–C and C–N stretches in the 1200–1500 cm^{-1} range. Net S_2–S_1 decay is the dominant decay path for ZnTPP and CdTPP as well, but the process occurs at rates that exceed (in the case of CdTPP, they vastly exceed) those predicted by weak interstate coupling. Alternate mechanisms for the radiationless decay of the S_2 states of ZnTPP and CdTPP have been explored. Large spin–orbit coupling constants and the presence of multiple, near-equiergic triplet states suggest that S_2–T_n intersystem crossing might occur at rates competitive with internal conversion. However, the measured efficiencies of S_2–S_1 internal conversion show that, at most, only a few percent of the S_2 population of ZnTPP and no more than about 30% of the S_2 population of CdTPP can decay by a "dark" path such as intersystem crossing.

Introduction

Metalloporphyrins are ubiquitous in nature,[1] are routinely used in photodynamic therapy,[2] and are of emerging use in practical photon-actuated devices such as photoactivated oxygen pressure sensors[3] and organic photovoltaic solar cells.[4] The photophysical and photochemical properties of the relatively long-lived triplet and lowest excited singlet states of these substances have therefore been thoroughly studied.[5] Complementary studies of the photophysical properties of their supramolecular arrays,[6] their solid-state aggregates,[7] and their analogues with modified macrocycles[8] are the subject of intense ongoing interest.

By comparison, relatively little is known about the photophysical behavior of the higher excited electronic states of even well-established model diamagnetic metalloporphyrins such as zinc tetraphenylporphyrin (ZnTPP, *meso*-tetraphenylporphine zinc), its analogues such as MgTPP and CdTPP, and simple *β*-substituted derivatives such as zinc octaethylporphyrin (ZnOEP). The higher excited states of such molecules have assumed greater importance recently, owing to their proposed involvement in photovoltaic cells (with photon upconversion by triplet–triplet annihilation[9]), their potential use in optically activated molecular logic devices,[10] and the more general need to understand the behavior of materials under intense laser excitation. Two recent reviews of the electronic spectroscopy and photophysics of Soret-excited metalloporphyrins (and of the more highly excited states of other chromophores) describe our current state of knowledge in some detail.[11] The background to the important open questions to be addressed in this paper is summarized below.

The identities of the electronic states accessed following one-photon excitation of diamagnetic metalloporphyrins such as MgTPP, ZnTPP, and CdTPP in their Soret and higher energy absorption bands are still very much an open question. The Soret band dominates the near-UV blue region of the absorption spectrum; in D_{4h} symmetry, the transition is 2^1E_u–$^1A_{1g}$ and has an oscillator strength approaching unity. However, one-photon transitions to gerade excited states of similar or higher energy are strongly electric dipole forbidden; such states, if present, will therefore be optically dark and accessible with reasonable quantum efficiency only by two-photon excitation from the ground state,[12] by one-photon optical excitation of the lowest excited singlet state,[13] or by radiationless relaxation following initial one-photon excitation to still higher ungerade states. A recent transient absorption study by Schalk et al.[13] has shown that gerade states do exist at energies near those accessible by excitation in the Soret bands in several free base and zinc porphyrins, but their involvement in the relaxation of higher ungerade states has not been demonstrated. Similarly, higher triplet states will be difficult to observe except by triplet–triplet absorption[14] from the long-lived lowest triplet, 1^3E_u, but can be populated by intersystem crossing following initial excitation in the Soret region. TD-DFT calculations show that at least six triplet states lie at energies between those of the two lowest excited ungerade singlet states.[15] However, almost nothing is known about their participation in the radiationless decay of the electronic states of the porphyrins populated upon one-photon excitation in the UV blue region.

Scant, but nevertheless convincing, experimental evidence suggests that states other than the 2^1E_u (S_2) and 1^1E_u (S_1) states are involved in the radiationless relaxation of metalloporphyrins populated upon one-photon excitation in the Soret band. Yu, Baskin, and Zewail,[12b] for ZnTPP in benzene, observed distinctly

* To whom correspondence should be addressed. Phone: (306) 966-4667. Fax: (306) 966-4730. E-mail: ron.steer@usask.ca.

Photophysics of Soret-Excited Tetrapyrroles in Solution

J. Phys. Chem. A, Vol. 112, No. 26, 2008 **5825**

different relaxation dynamics when exciting directly by one-photon absorption to 2^1E_u compared that with two-photon excitation to higher states. They also reported that, contrary to the previous report of Mataga et al.,[16] the 2^1E_u fluorescence decay time of ZnTPP was measurably longer than the rise time of the 1^1E_u state's fluorescence. They postulated that the Soret absorption band consists of transitions from S_0 to two manifolds of states with distinctly different electronic and vibrational couplings to S_1 and higher states and invoked a state designated as S_2' in near resonance with S_2 to account for their observations. Later, Karolczak, et al.[17] and Lukaszewicz, et al.[18] demonstrated that, although S_2 - S_1 internal conversion is the major radiationless decay process when ZnTPP is excited in the Soret region, the quantum yield of this process is measurably less than one and is a function of both excitation wavelength and solvent. A small but significant fraction of S_2's population decays by a route that by-passes S_1, in apparent support of the presence of an S_2' state. Nevertheless, Velate et al.[19] showed that the rates of S_2–S_1 internal conversion of ZnTPP in a wide range of solvents were apparently consistent with the expectations of the energy gap law of radiationless transition theory, despite the fact that the two coupled states are of the same symmetry. In summary, the nature of the additional state(s) involved in the radiationless relaxation of Soret-excited metalloporphyrins such as ZnTPP, the model meso-substituted compound, remains rather uncertain.

In addition, Liu, et al.[15] have shown that common, β-substituted diamagnetic metalloporphyrins such as ZnOEP exhibit S_2 radiationless decay rates that are orders of magnitude faster than those expected on the basis of the weak coupling behavior of the meso-substituted metalloporphyrins such as ZnTPP. Thus, the effect of different substitution patterns on the mechanism(s) and rates of radiationless decay of the S_2 states of these common model systems is also unclear.

We have undertaken to investigate further the radiationless relaxation of the higher excited electronic states of simple, model diamagnetic metalloporphyrins using both steady-state and fast time-resolved methods. Here, we report the results of experiments on the series of tetraphenylmetalloporphyrins, MTPP (M = Mg, Zn, Cd), in a wide variety of solvents, evaluate the applicability of the weak coupling model to S_2–S_1 internal conversion, and evaluate the importance of radiationless relaxation of the S_2 states of these compounds via their upper triplet states, T_n ($n > 2$).

Experimental Section

Materials. The three title compounds, M(II) *meso*-tetraphenylporphyrin (MTPP, M = Mg, Zn, Cd), were purchased from Alfa Aesar (MgTPP), Sigma-Aldrich (ZnTPP, low chlorin), and Frontier Scientific Inc. (CdTPP). All compounds were checked for impurities by NMR and/or mass spectroscopy and were screened for fluorescent impurities, particularly the free base. They were used as received if no significant impurity fluorescence was detected. Ethanol (Commercial Alcohols, Inc.), fluorobenzene (Fluka, for spectroscopy), and all other solvents (Aldrich) were of the highest purity available and were stored over 3 or 4 Å molecular sieves.

Instrumentation. Picosecond S_2–S_0 fluorescence decay times and S_1–S_0 fluorescence rise times of the MTPP samples were measured using the fluorescence upconversion setup shown schematically in Figure 1. The femtosecond laser source was a Ti:sapphire laser (Coherent, Vitesse Duo) and regenerative

amplifier (Coherent, RegA 9000), operating at a 100 kHz repetition rate with an output average power of ~400 mW at 800 nm.

The output of the RegA was passed through an 80/20 beam splitter. The larger fraction of the power at 800 nm served as the gate pulse for sum-frequency generation after passing the pulse train through a variable delay line (Newport, ILS150PP controlled by an ESP 300 motion controller) and focusing it with a 400 mm focal length planoconvex lens onto the sum-frequency crystal used for upconversion. The smaller fraction of the of 800 nm beam was passed through a 0.5 mm thick type I BBO crystal (Photop, UTO8201) at a phase-matching angle of 29.2°, generating the second harmonic at 400 nm. The 400 nm pump beam was then passed through a fixed delay and a half-wave ($\lambda/2$) plate and focused by a first surface Al-coated 90° off-axis parabolic mirror (Edmund Optics, effective focal length = 101 mm) into the sample. The sample was continuously flowed through a 200 μm thick quartz cell (Starna); the flow rate was controlled by a HPLC pump (Millipore, Model 510). The fluorescence from the sample was collected with a combination of two planoconvex lenses (each with a 50 mm focal length) and focused into a 0.5 mm thick type I BBO crystal (Photop, UTO8201), to generate, together with the gate pulse, the sum frequency at a phase-matching angle of 38°. The angle between the gate and pump beams was held at ~10° to achieve maximum overlap in the BBO crystal. The upconverted light was passed through a filter to remove scattered gate and pump light and was focused (with a 50 mm focal length planoconvex lens) onto the entrance slit of a double monochromator (CM112, Spectral products). The signal at the user-selected sum frequency ($1/\lambda_{sum} = 1/\lambda_{em} + 1/\lambda_{gate}$) was detected by a photomultiplier (Hamamatsu, H7732P-01 module with C7169 power supply) connected to a two-channel gated photon counter (Stanford Research Systems, SR400) via a preamplifier (Stanford, SR445). The data acquisition, delay, and monochromator systems were controlled by an in-house program written in Labview. With the instrumentation described above, pump-gate cross-correlation traces were near Gaussian, with a full width at half-maximum (fwhm) of ~170−230 fs.

Steady-state absorption spectra of the MTPP samples in various solvents were measured with a Varian−Cary 500 spectrophotometer. The corresponding fluorescence emission and fluorescence−excitation spectra were measured with either a Jobin−Yvon Spex Fluorolog instrument or a Photon Technology International QuantaMaster spectrofluorometer fitted with double monochromators on both the excitation and emission arms and a calibrated photodiode for correcting the excitation spectra. Care was taken to calibrate these instruments and to use them only in their regions of linear response. When comparing steady-state absorption and fluorescence excitation spectra, care was taken to measure both under identical conditions of excitation and emission bandwidth (typically $\Delta\lambda_{em} = \Delta\lambda_{ex} = 1.8$ or 2.0 nm). The emission spectra were corrected synchronously using emission detector sensitivity correction files provided by the manufacturer and preinstalled in the spectrofluorometer's data acquisition software.

Methods. We have demonstrated[15,19] that ZnOEP must have an S_2 population decay time of less than ~50 fs (and a best estimate of 20 fs). We therefore have employed the observed S_2–S_0 emission of ZnOEP in benzene to obtain the instrument response function (IRF) for our system at the wavelength of maximum fluorescence intensity of our samples. This function has a fwhm of ~470 fs and is well-modeled by a Gaussian cross-correlation function, symmetrically broadened by the fluores-
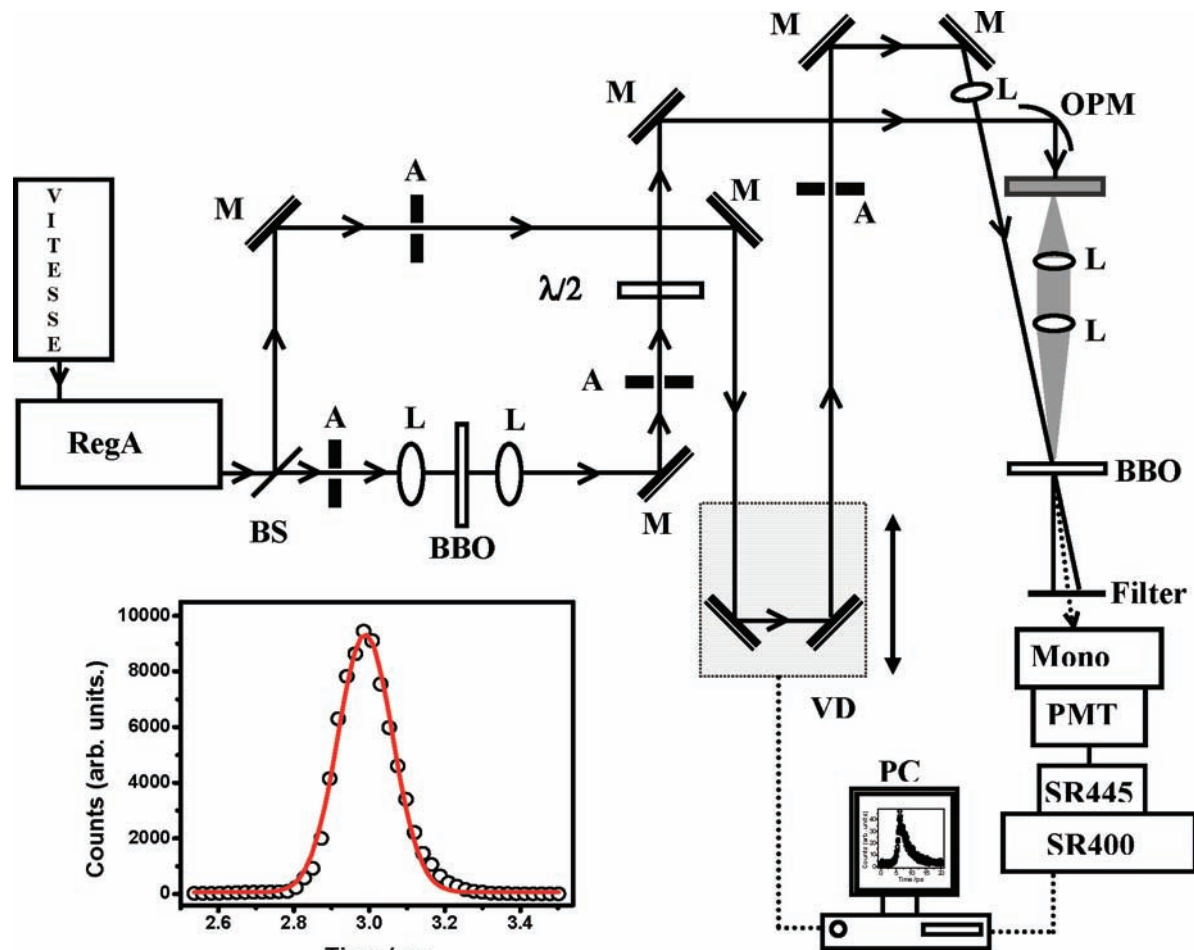
Figure 1. Schematic diagram of fluorescence upconversion equipment with cross-correlation trace, lower left. M, mirror; A, aperture; BS, beam splitter; L, plano convex lens; VD, variable delay; OPM, off-axis parabolic mirror; Mono, monochromator.

cence collection optics employed and convoluted with a fast exponential decay. Using a similar fluorescence upconversion system, Zewail and co-workers[12a] have shown that the free base tetraphenyl porphine (H$_2$TPP) in benzene exhibits an S$_2$ population decay time of ~30 fs. When we observe the temporal S$_2$ fluorescence profile of H$_2$TPP under similar conditions, we routinely obtain an emission profile that is about 30 fs wider than that of ZnOEP, in semiquantitative agreement with Zewail's measurement and justifying the use of the temporal S$_2$–S$_0$ emission profile of ZnOEP as our instrument response function.

Previous S$_2$ decay and S$_1$ rise measurements on ZnTPP using similar fluorescence upconversion instrumentation have shown that intramolecular vibrational relaxation processes in these systems are complete within the first 200 fs following excitation.[12,16] Both MgTPP and ZnTPP exhibit S$_2$ population decays and S$_1$ population rise times in the $3.5 \geq \tau \geq 1.3$ ps range in all solvents employed in this study. In order to avoid complications due to intramolecular vibrational relaxation, fits of the temporal emission profiles for these two molecules were made for $t > 200$ fs. Fits of single exponential functions to the S$_2$ emission decays at $t > 200$ fs yielded no significant difference in the lifetime compared with those obtained by full deconvolution. For the S$_2$ emission decay of CdTPP, lifetimes in the <250 fs range were obtained solely by deconvolution. The S$_1$ emission rise times were obtained by fitting the observed S$_1$ emission profile to a function consisting of one fast exponential rise and two longer exponential decays. The two decays were (i) on the order of 10–20 ps, corresponding to intermolecular

vibrational relaxation of the S$_1$ state and (ii) on the order of several nanoseconds, corresponding to S$_1$ population decay. These observations and fitting parameters are in complete agreement with previous studies on ZnTPP in benzene[12] and ethanol.[16]

A dilute solution of ZnTPP in ethanol ($c = 0.5 \mu$M) was used as a reference when calculating the relative S$_2$–S$_0$ emission quantum yields of other samples. To minimize errors in the determination of relative emission quantum yields, the absorbances of the dilute sample and reference solutions were adjusted so that they were almost identical at the wavelength(s) used for excitation in the Soret region. All samples of ZnTPP in different solvents were excited at 400 nm, whereas the excitation wavelength for CdTPP was set at 410 and 405 nm for MgTPP (i.e., to the blue of the S$_2$–S$_0$ maximum in all cases to minimize interference from scatter of the excitation light).

The measured fluorescence spectra were subjected to the following corrections before using the fluorescence intensity data to calculate emission quantum yields. First, the raw background spectrum was corrected by multiplying it by the constant correction factor $F = (1 - 10^{-A_{ex}})/(2.303A_{ex})$, where A_{ex} is the absorbance of the sample (or reference) solution at the excitation wavelength, to account for the reduced incident intensity of the incident light as it traverses the cell. The corrected background emission spectrum (due to solvent Raman scattering and any baseline drift) was then subtracted from the measured emission spectrum. When using different excitation wavelengths for the sample and reference (rare), the incident intensity differences
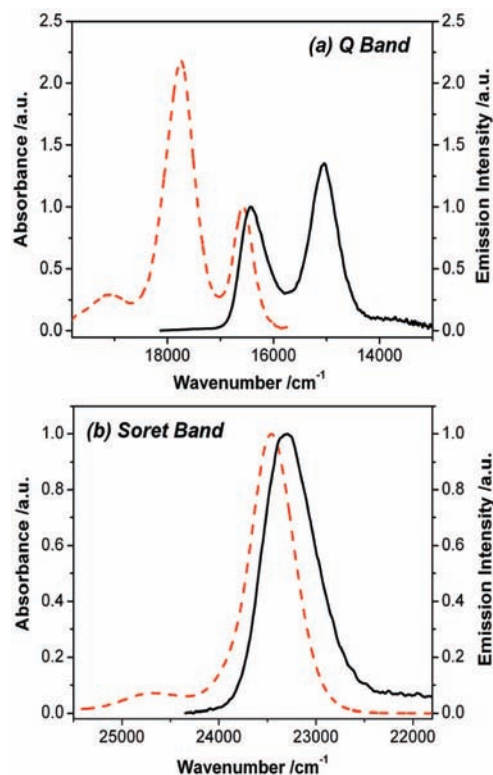
Photophysics of Soret-Excited Tetrapyrroles in Solution

J. Phys. Chem. A, Vol. 112, No. 26, 2008 **5827**

Figure 2. Absorption ($- - -$) and emission ($-$) spectra of MgTPP in benzene ((a) Q band and (b) Soret band), with the excitation wavelength at 405 nm and $c = 0.5$ μM at room temperature.

Figure 3. Normalized S_2-S_0 absorption spectrum ($- - -$) and corrected emission excitation spectrum ($-$) of MgTPP in toluene, $c = 0.4$ μM, obtained by observing S_1-S_0 emission at 663 nm.

were accounted for by using a calibrated photodiode preinstalled in the PTI spectrofluorometer. Because the overlap between the S_2-S_0 absorption and corresponding emission bands is extensive, care was taken to avoid artifacts (due to the inner-filter effect) that would influence the shape and position of the emission band and the magnitude of the fluorescence quantum yields. These artifacts were minimized by using dilute solutions in 10 mm × 2 mm cuvettes (Hellma), with excitation along the long path and emission exiting along the short path. When using dilute solutions, further corrections of the emission spectra such as those described by us earlier[15] were unnecessary.

Relative S_2-S_0 fluorescence quantum yields were calculated based on the corrected fluorescence spectra using the expression

$$\Phi_s = \Phi_r \times \frac{I_s^{em}}{I_r^{em}} \times \frac{F_r}{F_s} \times \frac{n_s^2}{n_r^2} \qquad (1)$$

where the reference is ZnTPP in ethanol ($\Phi_r = 1.42 \times 10^{-3}$ excited at 400 nm, Karolczak et al.[17]). Here, I is the integrated area of the fluorescence spectrum after correction; s and r represent the sample and the reference, respectively. F is the correction factor, given above, and n is the refractive index of the solvent.

All experiments were carried out in air-saturated dry solutions at room temperature.

Results and Discussion

The S_2-S_0 and S_1-S_0 absorption and emission spectra of dilute solutions of MgTPP, ZnTPP, and CdTPP were measured in several solvents of differing polarities and refractive indices. These spectra are not materially different from those previously reported.[20] Figure 2 is representative. Both absorption and emission spectra are mildly sensitive to solute concentration due
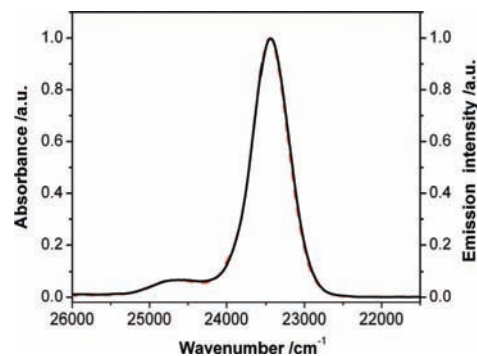
to porphyrin aggregation at higher concentrations; the effect is greater in the weakly solvating nonpolar solvents than in good solvents such as ethanol and DMF. Quantitative comparisons of the S_2-S_0 absorption spectra with the fluorescence–excitation spectra obtained by exciting dilute solutions in the Soret region and observing S_1 emission are particularly revealing. We have previously reported that the fluorescence–excitation spectra of ZnTPP obtained in this way exhibit slightly lower intensities than the corresponding absorption spectra on both the red side of the main Soret band and in its vibronic satellite to the blue.[17,18] However, using new instrumentation in the present measurements, we see no such effect for MgTPP in the same solvents and find the effect in ZnTPP to be somewhat less pronounced than previously reported.[17,18] Figure 3 shows that the S_2-S_0 absorption and the corrected S_2-S_0 fluorescence–excitation spectra of MgTPP, taken observing S_1-S_0 fluorescence, are superimposable when taken under identical conditions of spectral bandwidth and resolution. In dilute solutions of MgTPP, we therefore find no spectroscopic evidence of a second nonradiative relaxation process that bypasses S_1 and conclude that MgTPP differs from ZnTPP[17,18] in this respect. Both the S_2-S_0 and S_1-S_0 fluorescence quantum yields (vide infra) are much lower for CdTPP, making quantitative comparisons of its absorption and emission excitation spectra subject to greater error than those of MgTPP and ZnTPP.

It is nevertheless possible to measure accurately the relative intensities of S_1-S_0 fluorescence of pairs of these compounds when exciting at wavelengths in both the Soret and Q bands where the absorbances of the two solutions are identical, as shown in Figure 4 for MgTPP and ZnTPP in ethanol. Here, excitation of solutions of each of the two metalloporphyrins in the same solvent at the same wavelength and at the same absorbance in both the Soret and Q bands (417 and 559 nm for the MgTPP–ZnTPP pair) gives a ratio, $R_{MTPP} = I_S/I_Q$, of the S_1-S_0 emission intensity for exciting in the Soret band compared with direct excitation in the Q band for each compound. Because the effects of excitation wavelength and absorbed intensity are eliminated in these measurements, the ratio of ratios, R_{MgTPP}/R_{ZnTPP}, for the two compounds is equal to the ratio of the net S_2-S_1 internal conversion efficiencies (η_{ic}) in the two compounds, that is, $R_{MgTPP}/R_{ZnTPP} = \eta_{ic}(MgTPP)/\eta_{ic}(ZnTPP)$. The values of $\eta_{ic}(ZnTPP)$ have been reported previously[17,18] from measurements of absolute quantum yields of S_1-S_0 emission as a function of excitation wavelength in the Soret and Q bands and are slightly less than 1 at 417 nm, the Soret excitation wavelength used here for the MgTPP–ZnTPP pair. Similar measurements were also made for the ZnTPP–CdTPP pair. The results give $\eta_{ic}(MgTPP) = 1.00$, $\eta_{ic}(ZnTPP) = 0.93$, and $\eta_{ic}(CdTPP) = 0.69$, with an estimated error of
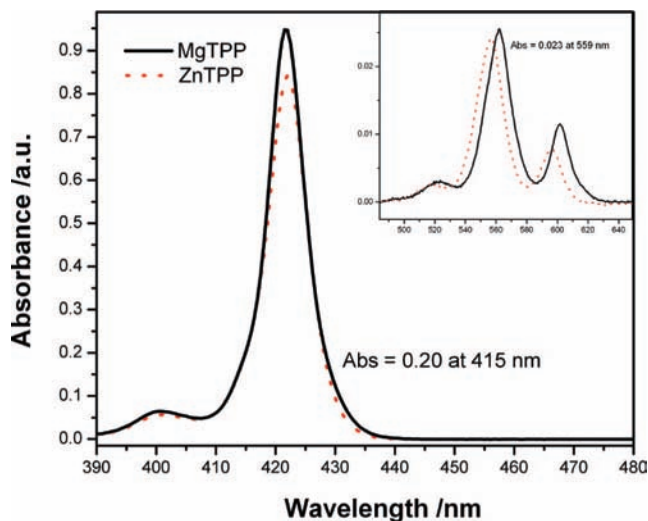
Figure 4. Absorption spectra of MgTPP and ZnTPP in ethanol showing wavelengths of overlap in the Soret and Q band regions where relative efficiencies of S_2–S_1 emission were measured.

TABLE 1: Spectroscopic Data for MTPP in Several Solvents at Room Temperature

MTPP	solvent	n	f_1	$E(S_1)$ (cm^{-1})	$E(S_2)$ (cm^{-1})	$\Delta E(S_2$–$S_1)$ (cm^{-1})
MgTPP	ethanol	1.362	0.222	16560	23650	7110
	1-propanol	1.385	0.234	16550	23600	7080
	1-butanol	1.399	0.242	16540	23560	7050
	DMF	1.428	0.257	16520	23470	6980
	fluorobenzene	1.465	0.276	16530	23410	6910
	benzene	1.501	0.295	16470	23350	6880
	toluene	1.503	0.296	16480	23360	6880
ZnTPP	ethanol	1.362	0.222	16689	23619	6930
	DMF	1.428	0.257	16637	23469	6832
	benzene	1.501	0.295	16866	23548	6682
CdTPP	ethanol	1.362	0.222	16284	23159	6875
	benzene	1.501	0.295	16210	22906	6696

± 0.05 in each case. The unit quantum efficiency of S_2–S_1 internal conversion for MgTPP is entirely consistent with the observation of overlapping absorption and fluorescence–excitation spectra for this compound when measuring the S_1–S_0 fluorescence intensity as a function of excitation wavelength in the Soret region.

The quantum yields of S_2–S_0 fluorescence, quantum efficiencies of S_2–S_1 internal conversion, and excited-state energies (obtained from the wavenumbers of intersection of the absorption and corrected normalized fluorescence emission spectra) were measured for dilute solutions of MgTPP and CdTPP and were remeasured for ZnTPP in several solvents using conventional steady-state methods. The data are collected in Table 1, which also contains the values of the refractive indices and Lorenz–Lorentz polarizability functions of the solvents. Figure 5 shows that the electronic S_2–S_1 electronic energy spacings of both MgTPP and ZnTPP are linear functions of the Lorenz–Lorentz polarizability function, $f_1 = (n^2 - 1)/(n^2 + 2)$, which extrapolate at $n = 1$, within experimental error, to the spacings measured for the bare molecules in supersonic expansions.[21] For ZnTPP, the intercept at $f_1 = 0$ is 7738 ± 55 cm^{-1}, as compared with 7752 cm^{-1} from supersonic jet spectroscopy.[22a] For MgTPP, in which solubility limited the range of solvents (and therefore the range of accessible values of $\Delta E(S_2$–$S_1)$) that could be used, the comparable values are 7832 ± 54 cm^{-1} compared with 7996 cm^{-1} from supersonic jet spectroscopy.[22b] The slopes of these plots are similar, as
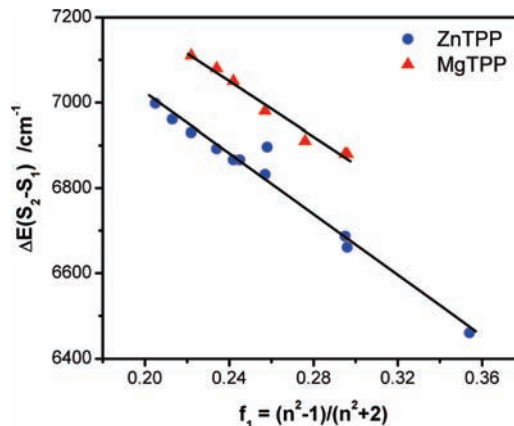

Figure 5. S_2–S_1 energy gap of MgTPP and ZnTPP as a function of the Lorenz–Lorentz polarizability function, $f_1 = (n^2 - 1)/(n^2 + 2)$. Data for ZnTPP from ref 19 are also included.

expected of two molecules with very similar structures. The solvatochromic effects observed in both MgTPP and ZnTPP are therefore due primarily to dispersive solute–solvent interactions, and the variation in $\Delta E(S_2$–$S_1)$ with solvent is due almost exclusively to the differences in the polarizabilities of the S_1 and S_2 states of the metalloporphyrin.

S_2 fluorescence decay times and S_1 fluorescence rise times were measured for solutions of MgTPP and ZnTPP in various solvents and of CdTPP in ethanol and benzene using femtosecond fluorescence upconversion. Fluorescence decay times as a function of the concentration of the solute were measured for test systems consisting of ZnTPP in ethanol and toluene. The measured decay curves became noisy at concentrations below about 50 μM but were all well-represented by single exponential functions and showed no significant systematic variation with solute concentration in the range of 50–300 μM in these "good" solvents. Because solute aggregates will be present in significant quantities at these solution concentrations,[17,18] we conclude that either the aggregates have the same S_2 fluorescence decay times as the monomers or, more likely, the aggregates have much lower fluorescence quantum yields of fluorescence at the observation wavelength and contribute little to the observed decays. The S_2 fluorescence decay profiles of ZnTPP in ethanol also showed no systematic variation with excitation laser power over the limited range of powers used in our studies, indicating that sequential two-photon absorption was likely not a significant problem in our measurements. Finally, also for ZnTPP in ethanol, no significant variation in the S_2 decay time was measured for different observation wavelengths within the Soret band when using a fixed excitation wavelength of 400 nm. Typical fluorescence decay curves for 150 μM MgTPP in ethanol and benzene excited at 400 nm are shown in Figure 6 and are similar in all respects to earlier ZnTPP fluorescence decays previously reported by us[19] and by others[12b,16] for excitation within the Soret band. Single exponential decay functions provide good fits to the measured decays over the entire range of concentrations for both solvents.

S_1 fluorescence rise times were measured for MgTPP and ZnTPP in three representative solvents; benzene, dimethylformamide, and ethanol. In all cases, the deconvoluted S_1 temporal fluorescence profiles were well-represented by multiexponential functions in which the rise times are identical to the corresponding S_2 decay times within an experimental error of no more than 10%. A typical pair of S_2 fluorescence decay and S_1 fluorescence rise plots, for MgTPP in ethanol, is shown in Figure 7. In all cases, the S_2 decay measurements produced data with
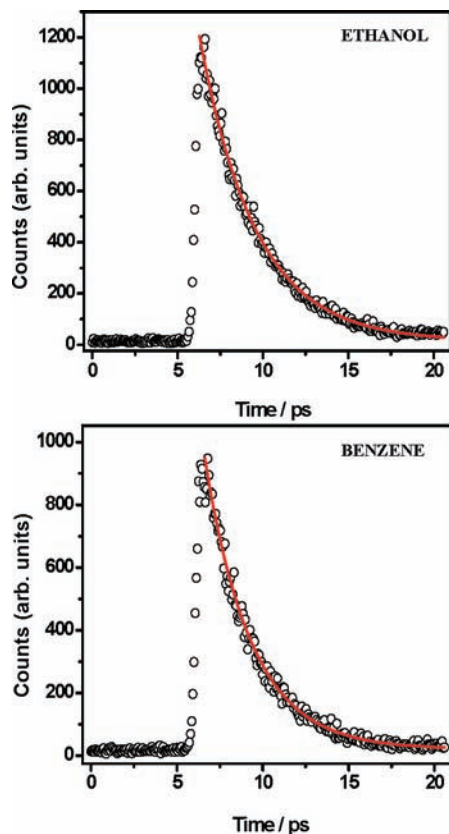
Photosphysics of Soret-Excited Tetrapyrroles in Solution

J. Phys. Chem. A, Vol. 112, No. 26, 2008 **5829**

Figure 6. Typical temporal S_2–S_0 fluorescence decays of MgTPP in ethanol (top, $\tau = 3.28$ ps) and benzene (bottom, $\tau = 2.71$ ps) at room temperature obtained by fluorescence upconversion. The solid line (red) shows the best fit of a single exponential decay function.
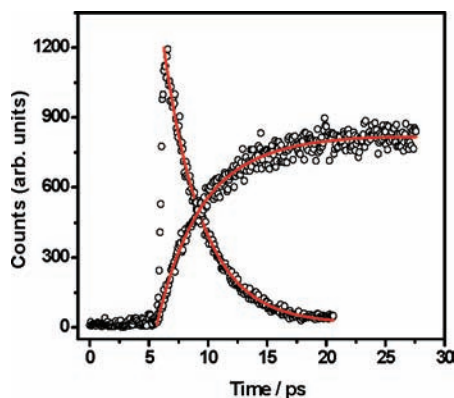

Figure 7. S_2 fluorescence decay ($\lambda_{em} = 433$ nm; $\tau_{decay} = 3.28$ ps) and S_1 fluorescence rise ($\lambda_{em} = 655$ nm; $\tau_{rise} = 3.25$ ps) profiles for MgTPP in ethanol, obtained with 400 nm excitation.

a greater signal-to-noise and lifetimes with a smaller relative error. These data are collected in Table 2, which also lists S_1 rise times in several representative solvents. The radiative and nonradiative decay constants for the S_2 states of both MgTPP and ZnTPP in all of the solvents investigated were calculated using the relationships $k_r = \phi_f/\tau$ and $\Sigma k_{nr} = (1 - \phi_f)/\tau$. The values of ϕ_f are all small enough that Σk_{nr} can be calculated directly from the inverse of the excited-state lifetime without loss of significant digits. These data are also collected in Table 2.

The measured S_2–S_0 fluorescence quantum yield of CdTPP is more than an order of magnitude smaller than those of MgTPP and ZnTPP, and its S_2 population decay time was too short to measure accurately using our fluorescence upconversion system.

An average value of $\tau(S_2) = 180 \pm 60$ fs was obtained for CdTPP in ethanol and benzene. The S_2–S_0 radiative decay constant, k_r, for CdTPP was also calculated from the measured $S_2 \leftarrow S_0$ absorption spectrum (in ethanol) using the integrated absorptivity method of Strickler and Berg,[23] and the S_2 lifetime of CdTPP was then obtained from k_r and the measured value of ϕ_f. The value obtained in this way is $\tau(S_2,\text{calc.}) = 115$ fs, which is in acceptable agreement with the experimental values obtained by fluorescence upconversion. Consequently, although the measured values of Σk_{nr} for MgTPP and ZnTPP are typically reproducible to within ~5% and have an absolute error of no more than twice this, the comparable value for CdTPP is subject to considerably larger error, nevertheless estimated to be no larger than 30%.

Of interest, we find no measurable difference between the S_2 fluorescence decay times and the S_1 fluorescence rise times for either MgTPP or ZnTPP in any of the solvents employed. Thus, we agree with Mataga et al.,[16] where we both measure $\tau = 2.35$ ps for both the S_2 decay and S_1 rise times of ZnTPP in ethanol, but we disagree with Yu et al.,[12b] who measured an S_2 decay time of 1.45 ps and an S_1 rise time of 1.15 ps for ZnTPP in benzene. For ZnTPP in benzene, we find the same S_2 decay time as Yu et al.[12b] but find no significant difference between it and the S_1 rise time. However, our fluorescence upconversion system has a slightly poorer time resolution than that used by Yu et al.,[12b] and it certainly produces S_1 rise time profiles with a lower signal-to-noise ratio. We can therefore neither definitively refute nor support the report that the S_1 rise time for ZnTPP in benzene is measurably faster than its S_2 decay time, and we can offer no useful comment on the previous interpretation[12b] that the difference may be due to the presence of a dark S_2' state in the vicinity of S_2 in benzene. We do note, however, that we see no significant difference between the S_2 decay times and the S_1 population rise times in either MgTPP or ZnTPP in any of the solvents investigated by us (Table 2).

Time-dependent perturbation theory provides the basis for understanding the relationship between molecular structure and the measured rates of radiationless decay of the excited electronic states of polyatomic molecules. The fundamental relationship describing the temporal probability of irreversible radiationless relaxation from an initial state $\langle S_i|$ to a weakly coupled final state $|S_f\rangle$ is given by the Fermi golden rule expression

$$k_{nr} = \frac{2\pi}{\hbar} C^2 F' \tag{2}$$

where $C = \langle S_i|H'|S_f\rangle$ is the interstate coupling energy, and F' is the corresponding density-of-states-weighted average Franck–Condon factor. Englman and Jortner[24] have provided the basis for correlating the nonradiative decay rate of a given excited state with ΔE, the electronic energy spacing between the two coupled states, in what is now called the energy gap law of radiationless transition theory. They derive eq 3

$$k_{nr} = \left\{ \sqrt{2\pi} C^2 / \hbar (\hbar \omega_M \Delta E)^{1/2} \right\} \exp\{ -(\gamma/\hbar \omega_M) \Delta E \} \tag{3}$$

where

$$\gamma = \ln\{ 2\Delta E / \sum_M \hbar \omega_M \Delta_M^2 \} - 1 \tag{4}$$

For S_2–S_1 internal conversion, C is the vibronic coupling matrix element, whereas for S_2–T_n intersystem crossing, C will be the molecule's effective spin–orbit coupling energy. In eqs 3 and 4, ω_M and Δ_M are the (angular) frequencies and reduced displacements of the accepting modes in the final state. For

TABLE 2: S_2 Fluorescence Lifetimes, S_2 Fluorescence Quantum Yields, and Rate Constants of Radiationless and Radiative Decay of MTPP in Several Solvents at Room Temperature

porphyrin	solvent	$\phi_f(S_2-S_0)$ /10^{-3}	$\tau(S_2)^a$ (ps)	Σk_{nr} /10^{11} s^{-1}	k_r /10^8 s^{-1}
MgTPP	ethanol	2.4	3.28 ± 0.07 (3.25)	3.05	7.3
	1-propanol	2.4	3.23 ± 0.07	3.10	7.7
	1-butanol	2.8	3.14 ± 0.06	3.18	8.9
	DMF	2.6	3.09 ± 0.08 (3.07)	3.24	8.4
	fluorobenzene	2.4	2.82 ± 0.06	3.55	8.5
	benzene	2.5	2.71 ± 0.07 (2.69)	3.69	9.2
	toluene	2.3	2.55 ± 0.06	3.92	9.0
ZnTPP	ethanol^b	1.42^b	2.35 (2.34)	4.26	5.91
	DMF	1.5	2.05 (2.07)	4.88	7.3
	benzene	1.2	1.49 (1.41)	6.71	8.0
CdTPP	ethanol	0.14	0.19 ± 0.06	53	7.4
	benzene	0.065	0.17 ± 0.06	59	3.8

^{a} Numbers in parentheses are S_1 rise times in representative solvents. ^{b} Reference standard (ref 17).
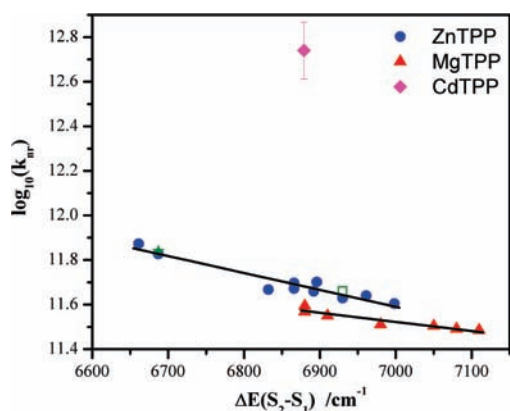

Figure 8. Energy gap law plots for MgTPP and ZnTPP, assuming that S_2-S_1 internal conversion is the sole S_2 radiationless decay process. Data for ZnTPP from refs 12b (☆), 16 (□), and 19 are also included.

radiationless transitions in the alternant aromatic hydrocarbons, the accepting modes are usually taken to be the group of C–H stretching modes with $\hbar\omega_M \sim 3000$ cm^{-1} because these modes have the largest Franck–Condon factors. However, for the nonalternant aromatic compound, azulene (the importance of which will be seen later), Griesser and Wild[25] have demonstrated that the appropriate accepting modes are the group of skeletal C–C stretches having an average $\hbar\omega_M = 1580$ cm^{-1}. This approach and the validity of the weak coupling model were later verified for azulene and a group of substituted azulenes in a variety of solvents by Tétreault et al.[26a] and Wagner et al.[26b] Graphs of $\log_{10}(k_{nr})$ versus ΔE are referred to as energy gap law plots; values of the parameter γ are obtained from their slopes after selecting an appropriate average value of $\hbar\omega_M$ as an adjustable parameter.

Figure 8 shows the energy gap law plots of $\log_{10}(k_{nr})$ versus $\Delta E(S_2-S_1)$ for MgTPP and ZnTPP in all of the solvents examined to date. This figure also contains data for ZnTPP in benzene previously obtained by Yu, Baskin, and Zewail[12b] and for ZnTPP in ethanol by Mataga et al.[16] Both points fall squarely on the line obtained by us in a preliminary report[20] and with the linear correlation using an extended data set obtained in the present study. Also included in Figure 8 is the datum for CdTPP obtained by the measurement described above. Note that both MgTPP and ZnTPP show good apparent linear energy gap law plots when it is assumed that S_2-S_1 internal conversion is the (major) nonradiative decay path for the Soret-excited molecules in all solvents. However, the slope and intercept of the plot for MgTPP are distinctly different from those for ZnTPP; the data are given in Table 3. Although previous reports

based on both calculation[27] and experiment[28] have attempted to fit the data for both MgTPP and ZnTPP with a single energy gap law correlation, Figure 8 clearly shows that different correlations are required for these two molecules. In solvents for which measurements of the S_2 fluorescence decays of both MgTPP and ZnTPP could be made for the same energy gap (i.e., at ΔE between about 6850 and 7000 cm^{-1}), the nonradiative decay rates for ZnTPP are significantly larger than those of MgTPP. The value of $\Delta E(S_2-S_1)$ for CdTPP in ethanol is similar, 6875 cm^{-1}, and CdTPP's S_2 nonradiative decay rate at this energy gap is about an order of magnitude larger still.

Values of γ for MgTPP and for ZnTPP obtained from the slopes of the energy gap law plots in Figure 8 have been used to calculate the apparent interstate coupling energy, C. The following relationship is derived by differentiation of $\log_{10}(k_{nr})$, from eq 3, with respect to $\Delta E(S_2-S_1)$

$$\frac{d(\log_{10}(k_{nr}))}{d(\Delta E)} = -\frac{1}{4.6\Delta E} - \frac{\gamma + 1}{2.3\hbar\omega_M} \quad (5)$$

Although the first term in eq 5 is often neglected,[25,27,28] there is no need to do so here where we are particularly interested in finding the values of γ and C at a fixed value of ΔE. We have chosen to evaluate γ at a value of $\Delta E = 6875$ cm^{-1} (the S_2-S_1 spacing for CdTPP in ethanol) so that the variation in the energy gap can be eliminated as a variable in analyzing the data for MgTPP, ZnTPP, and CdTPP. We have done so using the measured slopes of the energy gap law plots for three different assumed values of $\hbar\omega_M = 3000$, 1580, and 1350 cm^{-1}, corresponding to a typical C–H stretch, aromatic in-plane C–C stretch, and tetrapyrrole in-plane C–N or C–C stretch. (The vibrational frequencies in S_1 are assumed here to be similar to those in the ground state. The latter frequency also corresponds to the spacing between the two vibrational envelopes in the S_2-S_0 absorption and emission spectra.) The values of C are then determined by substituting the appropriate values of γ, ΔE, $\hbar\omega_M$, and k_{nr} into eq 3. The intercepts, A, of the energy gap law plots at $\Delta E = 0$ are also significant[24] and are obtained directly from extrapolation. The results are summarized in Table 3. In this table, crude estimates of γ and C for CdTPP are obtained by using the same energy gap law plot parameters for CdTPP as those of ZnTPP.

It is instructive to see how the energy gap law plots and the values of γ and C obtained from them compare not only among the MgTPP, ZnTPP, and CdTPP series but also with other chromophoric systems for which comparable S_2-S_1 radiationless relaxation data are available.[11a] Azulene and its simply substituted derivatives are useful comparators because, like the

Photophysics of Soret-Excited Tetrapyrroles in Solution

J. Phys. Chem. A, Vol. 112, No. 26, 2008 **5831**

TABLE 3: Energy Gap Law Parameters and Calculated Values of γ and C_{ic} for S_2–S_1 Internal Conversion

system	slope (cm)	intercept	$\hbar\omega$ (cm^{-1})	$\Delta E(S_2-S_1)$ (cm^{-1})	γ	$C_{ic}{}^a$ (cm^{-1})
azulenes	-4.0×10^{-4}	14.46	3000	15000	1.65	167
			1580		0.40	12
MgTPP	-4.1×10^{-4}	14.38	3000	6875	1.64	498
			1580		0.38	114
			1350		0.18	76
ZnTPP	-7.6×10^{-4}	16.91	1580	6875	(1.65)	(2.1×10^3)
			1350		(1.27)	(1.4×10^3)
CdTPP^b	–	–	1580	6875	(1.65)	(7.2×10^3)
			1350		(1.27)	(4.8×10^3)

^{a} Values in parentheses are calculated assuming (incorrectly) that S_2–S_1 internal conversion in ZnTPP and CdTPP can be described by the weak coupling case (see text). ^{b} Calculated for $k_{nr} = 5.6 \times 10^{12}$ s^{-1} and the energy gap law parameters for ZnTPP (see text).

MTPP, the states involved are all of π,π^* provenance.[25,26] Measurements of k_{nr} and ΔE obtained in previous investigations of azulene and its 1-fluoro and 1,3-difluoro derivatives in several solvents[26] have been used here to calculate the values of γ and C for S_2–S_1 internal conversion in this system at $\Delta E = 15000$ cm^{-1}. These values are also collected in Table 3. The most striking observations from these data are (i) that the slopes and intercepts of the azulene and the MgTPP energy gap law plots are identical within experimental error and (ii) the corresponding values of their intercepts at $\Delta E = 0$ and their vibronic coupling constants all fall within the limits expected[24] of the weak interstate coupling case of radiationless transition theory, that is, a pre-exponential factor, $A = 10^{(13 \pm 2)}$ and a singlet–singlet coupling constant $C \leq 10^3$ cm^{-1}. This is particularly important because it is well-established[25,26] that S_2–S_1 internal conversion in azulene occurs with unit efficiency and is adequately described by the weak coupling case of radiationless transition theory, as expected when the two coupled states are widely spaced ($\Delta E(S_2-S_1) \sim 15000$ cm^{-1}) and of different electronic symmetry ($^1A_1$ and $^1B_2$).

The values of γ obtained from the energy gap law plot for MgTPP require comment because they are unusually small. These small values of γ can readily be rationalized if the sum in eq 4 is taken over a large number of accepting vibrational modes in the S_1 state. The vibrational spectra of metalloporphyrins in their ground electronic states have been measured and the observed frequencies and their degeneracies assigned in detail.[29] We focus on the in-plane C–C and C–N stretches that lie in the 1200–1500 cm^{-1} range and assume that, consistent with the small Stokes shifts observed in MgTPP, vibrational frequencies assigned to the ground state can also be applied to the excited state without significant error. Following the analysis of Stein et al.,[29] we consider the phenyl groups of MgTPP to act as in-plane point masses. Using this model, there are a total of 71 in-plane vibrational modes, at least 20 of which are C–C and C–N stretches with wavenumbers in the 1200–1500 cm^{-1} range and an average of $\sim$1410 cm^{-1}. The latter value is remarkably close to the 0–0 to 0–1 spacing of the vibrational structure in the electronic spectra of these compounds and the value of $\hbar\omega_M = 1350$ cm^{-1} used for obtaining the best fit of the measured S_2–S_1 radiationless decay constants of MgTPP using the energy gap law. If we sum over $M \geq 20$ vibrations in eq 4 we find that Δ_M, the dimensionless displacement parameter, takes on a value of $\leq$0.3, exactly as required by the energy gap law analysis of Englman and Jortner[24] for the weak coupling regime. We also note that these calculations are not particularly sensitive to the exact number of modes or to the average vibrational wavenumber used in the calculation, as long as those in the 1200–1600 cm^{-1} range are employed.

All of the available experimental data therefore suggest that S_2–S_1 interaction in MgTPP can be described perfectly well by the weak vibronic coupling case of radiationless transition theory, despite the fact that the two coupled states are of the same symmetry (^1E_u in D_{4h}). The implication is that, in MgTPP, the two states are nested in such a way that only weak coupling occurs between them.

Knowing that S_2–S_1 internal conversion is the only significant radiationless process by which S_2 decays in MgTPP, we henceforth assume that that the weak coupling model applies in this case and that its values of A and C (Table 3) are characteristic of the internal conversion processes of all of the diamagnetic MTPP molecules at these values of ΔE. Then, if one also assumes that internal conversion is also the only radiationless process by which the S_2 states of ZnTPP and CdTPP decay, the values of A and C for ZnTPP and particularly those for CdTPP fall outside of the prescribed limits for weak coupling. The implication is that either S_2–S_1 internal conversion in ZnTPP and CdTPP is occurring by a strong(er) coupling pathway or that there is at least one additional parallel path by which S_2 can undergo competitive radiationless relaxation. Therefore, in Table 3, only the values of A, C, and γ for MgTPP can be interpreted in terms of a single internal conversion process in which the S_2 and S_1 states are weakly coupled.

We therefore now examine whether S_2–T_n intersystem crossing could be responsible for the increase in radiationless transition rates from the S_2 states of ZnTPP and CdTPP relative to that of MgTPP at the same energy. That is, we attempt to determine if at least two radiationless processes

$$S_2 \rightarrow S_1 \qquad k_{ic}$$
$$S_2 \rightarrow T_n \quad (2 < n < 9) \qquad k_{isc}$$
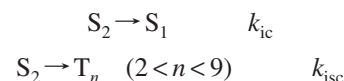
occur in parallel, with both contributing to the measured value of k_{nr}. We note first that TD-DFT (B3LYP/6-31G*) calculations[15] place six triplet states between the S_2 and S_1 states of ZnTPP; three of these lie within 0.1 eV of S_2. Second, we note that heavy-atom-enhanced S_1–T_n ($n = 1,2$) intersystem crossing in these same metalloporphyrins is responsible for the decrease in the lifetimes of their S_1 states from $\sim$8 ns in MgTPP to $\sim$2 ns in ZnTPP to $\sim$65 ps in CdTPP in similar solvents at room temperature.[20] The increases in these rates of S_1–T_n ($n = 1,2$) intersystem crossing scale semiquantitatively as the square of the spin–orbit coupling constants of the coordinated metal atoms. The group of $2 < n < 9$ triplet states contains every symmetry species characteristic of the D_{4h} point group except B_{1g}, and some are very nearly resonant with the S_2 state; therefore, stronger singlet–triplet interactions than those found in lower parts of the electronic manifold might be possible.

We therefore calculate the spin–orbit coupling constants for the MTPP molecules employed here and compare the data with

TABLE 4: Calculated Spin−Orbit Coupling Parameters and Maximum Values of k_{isc} for S_2-T_n Intersystem Crossing in MgTPP, ZnTPP, and CdTPP at Room Temperature

system	ζ_M (cm^{-1})	$\zeta_T = (\sum_i \zeta_i^2)^{1/2}$ (cm^{-1})	Σk_{nr} (s^{-1})	$k_{isc}(max) = \Sigma k_{nr}(1 - \eta_{ic})$ (s^{-1})	$(\zeta_T^2)_{rel}$[a]
MgTPP	40.9	161	3.6×10^{11}	$\leq 2 \times 10^{10}$ (<0.6)[a]	0.15
ZnTPP	389	418	4.8×10^{11}	3.4×10^{10} (1)[a]	1
CdTPP	1171	1.19×10^3	5.6×10^{12}	1.7×10^{12} (50)[a]	8.1

[a] Normalized to the values for ZnTPP = 1.

the values of C obtained from the energy gap law plot for MgTPP in which S_2-S_1 internal conversion is assumed to be the only significant S_2 radiationless decay process. The spin−orbit coupling constants for each atom in the MTPP molecules can be obtained from the multiplet splittings in their UV−visible absorption and emission spectra. The most appropriate method[30] of obtaining an upper limit for the spin−orbit coupling constant for the molecule, ζ_T, is to take the square root of the sum of the squares of the spin−orbit coupling constants for the individual atoms whose nuclei contribute fully to the relativistic process, that is

$$\zeta_T = \left(\sum_i \zeta_i^2\right)^{1/2}$$

The values of ζ_i for the Mg, Zn, and Cd atoms were obtained from the multiplet splittings of their $ns^2-ns^1np^1$ spectra,[31] whereas those of the H, C, and N atoms have been taken from previous reports.[30] The values of ζ_M for the individual metal atoms and of ζ_T for the MTPP compounds are given in Table 4. (The contributions from the more weakly coupled pendant phenyl groups have been fully weighted in the sum; the values of ζ_T in Table 4 should be taken as the upper limits of actual effective spin−orbit coupling constants in these molecules.) Note that for the three metalloporphyrins under study, $\zeta_{Mg} \ll \zeta_T$ for MgTPP, ζ_{Zn} contributes significantly to ζ_T for ZnTPP, and ζ_{Cd} is the dominant contributor to ζ_T for CdTPP. Note also that the upper limit values of ζ_T for MgTPP, ZnTPP, and CdTPP are all of the same order of magnitude or greater than the value of C for weak S_2-S_1 coupling in the internal conversion of MgTPP. This comparison, together with the close proximity of S_2 with states T_n (2 < n < 9) suggests that intersystem crossing to the triplet manifold could be competitive with S_2-S_1 internal conversion following excitation in the Soret bands of these compounds.

However, the measured values of η_{ic} presented above show that net S_2-S_1 internal conversion is the dominant decay path for these Soret-excited metalloporphyrins and that S_2-T_n intersystem crossing can at most contribute to only a fraction of S_2's decay in even the heaviest species, CdTPP. (Note that this assumes that back-intersystem crossing from T_n to the singlet manifold, which is improbable, is negligible). The maximum values of $k_{isc} = \Sigma k_{nr}(1 - \eta_{ic})$ are given in Table 4. Note that these values of k_{isc} do not scale even semiquantitatively with ζ_T^2 for the three compounds, MgTPP, ZnTPP, and CdTPP, when accurately known data for ZnTPP are used for normalization. We therefore conclude that pathways other than $S_2 - T_n$ intersystem crossing are most likely responsible for most of the enhanced rates of radiationless decay of the S_2 states of ZnTPP and CdTPP compared with that of MgTPP.

Alternate pathways that must be considered are (i) direct S_2-S_0 internal conversion, as has been observed in the upper excited singlet state manifold of the aromatic thiones[11a,32] and (ii) indirect $S_2-S_2'-S_0$ internal conversion via a "dark" state such as one of gerade parity or of charge-transfer character. Recent pump−probe studies by Schalk et al.[13] show that gerade

excited states could lie at suitable energies, perhaps between S_2 and S_1, in at least the zinc porphyrins. Thus, there is experimental evidence to support identifying S_2' with the "dark" 1^1E_g state, as we have previously suggested.[15,17,18] If irreversible, as is likely, such S_1 bypassing pathways can, however, account for only a small fraction of the net S_2 population decay in the MTPP systems investigated here. The large enhancements in the rates of S_2-S_1 internal conversion in ZnTPP and CdTPP compared with that for MgTPP cannot be explained by invoking either intersystem crossing or relaxation via a "dark" singlet state as a parallel decay process.

Conclusions

The photophysical behavior of three Soret-excited diamagnetic meso-substituted tetraphenylmetalloporphyrins, MgTPP, ZnTPP, and CdTPP, have been examined using both steady-state and femtosecond fluorescence upconversion methods. Only for MgTPP does the population decay rate of the S_2 state conform to the weak coupling case of radiationless transition theory and the energy gap law. For MgTPP in a variety of solvents, S_2-S_1 internal conversion occurs on a picosecond time scale with unit efficiency. The dominant accepting vibrational modes in the S_1 state are multiple in-plane C−C and C−N stretches in the 1200−1600 cm^{-1} range.

Net S_2-S_1 decay is the dominant decay path for ZnTPP and CdTPP as well, but the process occurs at rates that exceed (in the case of CdTPP, they vastly exceed) those expected on the basis of weak S_2-S_1 interstate coupling. Alternate mechanisms for the radiationless decay of the S_2 states of ZnTPP and CdTPP have been explored. The presence of multiple, near-equiergic triplet states and the magnitudes of spin−orbit coupling constants calculated from atomic spectra suggest that S_2-T_n intersystem crossing might occur at rates competitive with internal conversion. However, measured efficiencies of S_2-S_1 internal conversion show that, at most, only a few percent of S_2's population can undergo direct intersystem crossing to the triplet manifold in ZnTPP, and only about 30% can undergo direct intersystem crossing in CdTPP.

The following issues remain open. (i) Although the nonradiative decay of the S_2 state of MgTPP involves internal conversion to S_1 with unit efficiency and conforms well to weak S_2-S_1 coupling, the radiationless decay of the S_2 states of ZnTPP and CdTPP cannot be so described. A small (∼7%) fraction of the S_2 population of ZnTPP and about 30% of the S_2 population of CdTPP decay by a process or processes that bypass S_1. S_2-T_n (2 < n < 9) intersystem crossing is one of several process that might account for this "dark" pathway, but it cannot account for the enhanced rates of S_2-S_1 internal conversion in these compounds. A full description of the S_2-S_1 coupling mechanism in these heavier diamagnetic metalloporphyrins is not yet at hand. (ii) There is both calculational and experimental evidence for the presence of at least one dark state (S_2' of perhaps gerade parity) that lies near in energy to the S_2 (2^1E_u) state. The influence of such a state (or states) on the radiationless decay dynamics of the metalloporphyrins has not

Photophysics of Soret-Excited Tetrapyrroles in Solution

J. Phys. Chem. A, Vol. 112, No. 26, 2008 **5833**

been established. (iii) The rates of radiationless decay of the S_2 states of ZnOEP and perhaps those of other β-substituted metalloporphyrins have not been measured accurately but are much too fast to be described by weak S_2–S_1 coupling. However, no quantitative investigation of the influence of β-substitution on the photophysics of Soret-excited metalloporphyrins has been undertaken. (iv) A brief report of the lifetime of the S_2 state of zinc diphenylporphyrin is available,[16] but there has been no systematic study of the effects of reduction of the D_{4h} symmetry of the metalloporphyrin macrocycle by meso-substitution. The distinct out-of-plane location of the larger Cd atom in CdTPP and the resulting difference in metalloporphyrin symmetry should also be examined as a potential source of the enhanced rate of S_2–S_1 radiationless decay in CdTPP compared with that of ZnTPP and MgTPP. Part II of this series will address these questions.

References and Notes

(1) (a) Kadish, K. K.; Smith, K. M.; Guilard, R. *The Porphyrin Handbook*; Academic Press: San Diego, CA, 2000. (b) Dolphin, D. Ed. *The Porphyrins*; Academic Press: New York, 1978.

(2) (a) Szacillowski, K.; Macyk, W.; Drzewiecka-Matuszek, A.; Brindell, M.; Stochel, G. *Chem. Rev.* **2005**, *105*, 2647. (b) Donzello, M. P.; Ercolani, C.; Stuzhin, P. A. *Coord. Chem. Rev.* **2006**, *250*, 1530.

(3) Brinas, R. P.; Troxler, T.; Hochstrasser, R. M.; Vinogradov, S. A. *J. Am. Chem. Soc.* **2005**, *127*, 11851.

(4) (a) Nakano, A.; Osuka, A.; Yamazaki, T.; Nishimura, Y.; Akimoto, S.; Yamazaki, I.; Itaya, A.; Murakami, M.; Miyasaka, H. *Chem.—Eur. J.* **2001**, *7*, 3134. (b) Wagner, R. W.; Johnson, T. E.; Lindsey, J. S. *J. Am. Chem. Soc.* **1996**, *118*, 11166.

(5) For a review, see: Takagi, S.; Inoue, H. *Molecular and Supramolecular Photochemistry*; Ramamurthy, V., Schanze, K. S. Eds.; Marcel Dekker: New York, 2000; Vol. 5, p 215.

(6) (a) Nakamura, Y.; Aratani, N.; Osuka, A. *Chem. Soc. Rev.* **2007**, *36*, 831. (b) Song, H. E.; Kirmaier, C.; Schwartz, J. K.; Hintin, E.; Yu, L. H.; Bocian, D. F.; Lindsey, J. S.; Holten, D. *J. Phys. Chem. B* **2006**, *110*, 19121. (c) Collini, E.; Ferrante, C.; Bozi, R. *J. Phys. Chem. C* **2007**, *111*, 10636.

(7) Luo, L. Y.; Lo, C. F.; Lin, C. Y.; Chang, I. J.; Diau, E. W. G. *J. Phys. Chem. B* **2006**, *110*, 410, and references therein.

(8) (a) Ding, T.; Aleman, E. A.; Modarelli, D. A.; Ziegler, C. J. *J. Phys. Chem. A* **2005**, *109*, 7411. (b) Ventura, B.; Esposti, A. D.; Koszarna, B.; Gryko, D. T.; Flamigni, L. *New J. Chem.* **2005**, *29*, 1559.

(9) (a) Baluschev, S.; Miteva, T.; Yakutin, V.; Nelles, G.; Yasuda, A.; Wegner, G. *Phys. Rev. Lett.* **2006**, *97*, 143903. (b) Baluschev, S.; Yakutin, S.; Wegner, G.; Minsch, B.; Miteva, T.; Nelles, G.; Yasuda, A. *J. Appl. Phys.* **2007**, *101*, 023101. (c) Steer, R. P. *J. Appl. Phys.* **2007**, *102*, 076102/1.

(10) (a) Mirkin, C. A.; Ratner, M. A. *Annu. Rev. Phys. Chem.* **1992**, *43*, 719. (b) Remacle, F.; Speiser, S.; Levine, R. D. *J. Phys. Chem. B* **2001**, *105*, 5589. (c) Yeow, E. K. C.; Steer, R. P. *Chem. Phys. Lett.* **2003**, *337*, 391.

(11) (a) Burdzinski, G.; Kubicki, J.; Maciejewski, A.; Steer, R. P.; Velate, S.; Yeow, E. K. L. *Molecular Photochemistry and Photophysics*; Ramamurthy, V., Schanze K. S. Eds.; Taylor and Francis: New York, 2005; Vol. 14, p 1. (b) Tripathy, U.; Steer, R. P. *J. Porphyrins Phthalocyanines* **2007**, *11*, 228.

(12) (a) Baskin, J. S.; Yu, H.-Z.; Zewail, A. H. *J. Phys. Chem. A* **2002**, *106*, 9837. (b) Yu, H.-Z.; Baskin, J. S.; Zewail, A. H. *J. Phys. Chem. A* **2002**, *106*, 9845.

(13) Schalk, O.; Brands, H.; Balaban, T. S.; Unterreiner, A.-N. *J. Phys. Chem. A* **2008**, *112*, 1719.

(14) Tobita, S.; Kaizu, Y.; Kobayashi, H.; Tanaka, I. *J. Chem. Phys.* **1984**, *81*, 2962.

(15) Liu, X.; Yeow, E. K. L.; Velate, S.; Steer, R. P. *Phys. Chem. Chem. Phys.* **2006**, *8*, 1298.

(16) Mataga, N.; Shibata, Y.; Chosrowjan, H.; Yoshida, N.; Osuka, A. *J. Phys. Chem. B* **2000**, *104*, 4001.

(17) Karolczak, J.; Kowalska, D.; Lukaszewicz, A.; Maciejewski, A.; Steer, R. P. *J. Phys. Chem. A* **2004**, *108*, 4570.

(18) Lukaszewicz, A.; Karolczak, J.; Kowalska, D.; Maciejewski, A.; Ziolek, M.; Steer, R. P. *Chem. Phys.* **2007**, *331*, 359.

(19) Velate, S.; Liu, X.; Steer, R. P. *Chem. Phys. Lett.* **2006**, *427*, 295.

(20) Harriman, A. *J. Chem. Soc., Faraday Trans. 2* **1981**, *77*, 1281.

(21) Renge, I. *J. Photochem. Photobiol. A* **1992**, *69*, 135.

(22) (a) Even, U.; Magen, J.; Jortner, J.; Friedman, J.; Levanon, H. *J. Chem. Phys.* **1982**, *77*, 4374. (b) Even, U.; Magen, J.; Jortner, J.; Levanon, H. *J. Chem. Phys.* **1982**, *76*, 5684.

(23) Strickler, S. J.; Berg, R. A. *J. Chem. Phys.* **1962**, *37*, 814.

(24) Englman, R.; Jortner, J. *Mol. Phys.* **1970**, *18*, 145.

(25) Griesser, H. J.; Wild, U. P. *Chem. Phys.* **1980**, *52*, 117.

(26) (a) Tétreault, N.; Muthyala, R. S.; Liu, R. S. H.; Steer, R. P. *J. Phys. Chem. A* **1999**, *103*, 2524. (b) Wagner, B. D.; Tittlebach-Helmrich, D.; Steer, R. P. *J. Phys. Chem.* **1992**, *96*, 7904.

(27) (a) Kurabayashi, Y.; Kikuchi, K.; Kokubun, H.; Kaizu, Y.; Kobayashi, H. *J. Phys. Chem.* **1984**, *88*, 1308. (b) Ohno, O.; Kaizu, Y.; Kobayashi, H. *J. Chem. Phys.* **1985**, *82*, 1779. (c) Kobayashi, H.; Kaizu, Y. *Porphyrins: Excited States and Dynamics*; Gouterman, M., Rentzepis, P. M., Straub, K. D. Eds.; American Chemical Society: Washington, DC, 1986, p 105. (d) Kaizu, Y.; Asano, M.; Kobayashi, H. *J. Phys. Chem.* **1986**, *90*, 3906.

(28) (a) Gurzadyan, G. G.; Tran-Thi, T.-H.; Gustavsson, T. *J. Chem. Phys.* **1998**, *108*, 385. (b) Gurzadyan, G. G.; Tran-Thi, T.-H.; Gustavsson, T. *Proc. SPIE-Int. Soc. Opt. Eng.* **2000**, *4060*, 96.

(29) Stein, P.; Ulman, A.; Spiro, T. G. *J. Phys. Chem.* **1984**, *88*, 369. This analysis is confirmed by DFT calculations of the ground state vibrational wavenumbers.

(30) McGlynn, S. P.; Azumi, T.; Kinoshita, M. *Molecular Spectroscopy of the Triplet State*; Prentice-Hall: Englewood Cliffs, NJ, 1969.

(31) Bacher, R. F.; Goudsmit, S. *Atomic Energy States*; McGraw-Hill: New York, 1932.

(32) Maciejewski, A.; Steer, R. P. *Chem. Rev.* **1993**, *93*, 67.